
This is an electronic reprint of the original article.
This reprint may differ from the original in pagination and typographic detail.

Author(s): Lehtonen, Mikko & Genty, Goery & Ludvigsen, Hanne & Kaivola, Matti
Title: Supercontinuum generation in a highly birefringent microstructured fiber
Year: 2003
Version: Final published version

Please cite the original version:

Lehtonen, Mikko & Genty, Goery & Ludvigsen, Hanne & Kaivola, Matti. 2003. Supercontinuum generation in a highly birefringent microstructured fiber. *Applied Physics Letters*. Volume 82, Issue 14. 2197. ISSN 0003-6951 (printed). DOI: 10.1063/1.1565679.

Rights: © 2003 American Institute of Physics (AIP). This article may be downloaded for personal use only. Any other use requires prior permission of the author and the American Institute of Physics.
<http://scitation.aip.org/content/aip/journal/apl>

All material supplied via Aaltodoc is protected by copyright and other intellectual property rights, and duplication or sale of all or part of any of the repository collections is not permitted, except that material may be duplicated by you for your research use or educational purposes in electronic or print form. You must obtain permission for any other use. Electronic or print copies may not be offered, whether for sale or otherwise to anyone who is not an authorised user.

Supercontinuum generation in a highly birefringent microstructured fiber

M. Lehtonen, G. Genty, H. Ludvigsen, and M. Kaivola

Citation: *Applied Physics Letters* **82**, 2197 (2003); doi: 10.1063/1.1565679

View online: <http://dx.doi.org/10.1063/1.1565679>

View Table of Contents: <http://scitation.aip.org/content/aip/journal/apl/82/14?ver=pdfcov>

Published by the [AIP Publishing](#)

Articles you may be interested in

[Switchable Q-switched and modelocked operation in ytterbium doped fiber laser under all-normal-dispersion configuration](#)

Rev. Sci. Instrum. **86**, 033103 (2015); 10.1063/1.4913749

[Spectrally tailored supercontinuum generation from single-mode-fiber amplifiers](#)

Appl. Phys. Lett. **104**, 201112 (2014); 10.1063/1.4875911

[Single-polarization polarization maintaining optical fiber with large stress birefringence and high homogeneity](#)

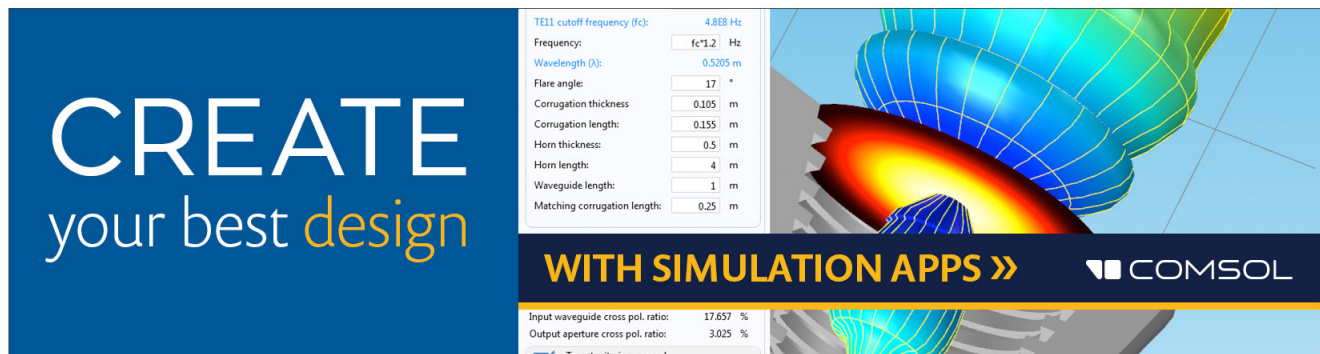
Appl. Phys. Lett. **89**, 101101 (2006); 10.1063/1.2345238

[Polarization mode dispersion: Characterization of optical fiber using cross-correlation interferometry](#)

Rev. Sci. Instrum. **76**, 123102 (2005); 10.1063/1.2136880


[Supercontinuum growth in a highly nonlinear fiber with a low-coherence semiconductor laser diode](#)

Appl. Phys. Lett. **85**, 4863 (2004); 10.1063/1.1818332



CREATE
your best design

TE11 cutoff frequency (fc): 4.8E8 Hz
Frequency: fc*1.2 Hz
Wavelength (lambda): 0.5205 m
Flare angle: 17 °
Corrugation thickness: 0.105 m
Corrugation length: 0.155 m
Horn thickness: 0.5 m
Horn length: 4 m
Waveguide length: 1 m
Matching corrugation length: 0.25 m

WITH SIMULATION APPS >> 

Input waveguide cross pol. ratio: 17.657 %
Output aperture cross pol. ratio: 3.025 %
 Target criterion: passed

Supercontinuum generation in a highly birefringent microstructured fiber

M. Lehtonen,^{a)} G. Genty, and H. Ludvigsen

*Fiber-Optics Group, Metrology Research Institute, Helsinki University of Technology,
P.O. Box 3000, FIN-02015 HUT, Finland*

M. Kaivola

*Department of Engineering Physics and Mathematics, Helsinki University of Technology,
P.O. Box 2200, FIN-02015 HUT, Finland*

(Received 28 October 2002; accepted 10 February 2003)

We present experimental results on supercontinuum generation in a highly birefringent microstructured fiber. We show that such a fiber offers clear advantages for continuum generation over weakly birefringent fibers. In particular, the polarization is preserved along the fiber for all the spectral components. Furthermore, the two eigenpolarizations exhibit different dispersion characteristics, which provide a convenient way of tuning the properties of the generated continuum. We investigate the impact of the pump wavelength and pulse duration on the continuum and use the results to generate an ultrabroadband continuum extending from 400 to 1750 nm. © 2003 American Institute of Physics. [DOI: 10.1063/1.1565679]

The recent introduction of optically highly nonlinear microstructured fibers (MFs) has enabled efficient generation of coherent supercontinuum radiation.¹ Such broadband radiation has already found several applications, e.g., in the fields of optical metrology,² sensor technology,³ and optical tomography.⁴ Keen interest has also been directed to understanding the physical mechanisms leading to the generation of the supercontinuum (SC) in MFs.^{5–10} It has been learned that the spectral properties of the SC critically depend on both the characteristics of the MF and the parameters of the pump pulses, i.e., wavelength, polarization, and pulse width. For short pump pulses on the order of tens of femtoseconds, the input pulse breaks up into multiple solitons. Soliton self-frequency shift with simultaneous emission of blueshifted dispersive waves subsequently leads to the formation of the continuum.^{6,7,10} In the previous studies, the experiments have been performed using weakly birefringent fibers. In this letter, we report on supercontinuum generation in highly birefringent fibers. The main advantage with these fibers is in the preservation of the state of polarization of the field propagating in the fiber.¹¹ For several applications, it is essential that the output has a well-defined polarization. In addition, the preserved polarization enhances the nonlinear interactions so that less power is required to generate the SC. Furthermore, the possibility to simultaneously generate two continua with orthogonal polarizations allows for an extra degree of freedom in tuning the properties of the SC.

In this work, we investigate the effects of pump laser wavelength, polarization, and pulse width on the SC generated in a highly birefringent MF. The experimental results and the analysis provide useful information that helps to optimize and tune the properties of the supercontinuum source.

The SC is generated by launching a train of ultrashort pulses from a mode-locked Ti:sapphire laser (Spectra Physics/Tsunami) into a highly birefringent microstructured fiber (Crystal Fibre A/S). The laser produces linearly polar-

ized femtosecond pulses at a repetition rate of 80×10^6 pps. A half-wave plate is used to vary the input polarization of the light pulses launched into the 5-m-long MF with an elliptical core of dimensions $1.5 \times 2.4 \mu\text{m}^2$ and a mode-field area of $2.3 \mu\text{m}^2$. The strong ellipticity of the core induces high birefringence, resulting in the preservation of the state of polarization of the pulses traveling in the fiber. The group delay (GD) and dispersion profiles of both the fast and slow principal axes of polarization of the fiber are shown in Fig. 1.¹² The dispersion of the fast (slow) axis is anomalous above the zero-dispersion wavelength (ZDW) of 635 (675) nm. The coupling efficiency into the fiber was 20%–30%. In the experiments we observe light at the output only in the fundamental mode, although theoretically the fiber should transmit at least three modes. The spectra at the output of the fiber were recorded with an optical spectrum analyzer (Ando 6315A) using a measurement bandwidth of 10 nm. The average output power P_{av} of the fiber was measured with a calibrated calorimeter.

The pump laser was tuned to the wavelengths 728, 771, and 810 nm. In each case, the input pulse duration T_{FWHM}

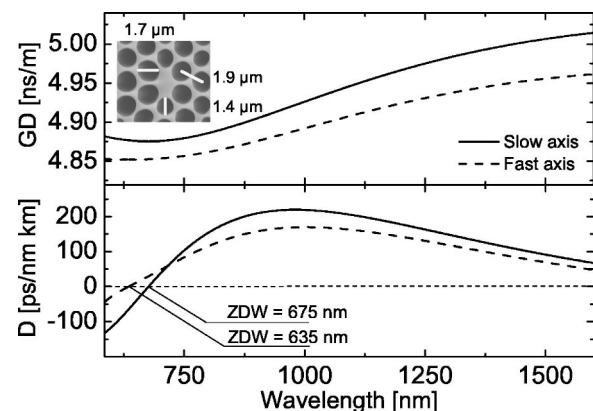


FIG. 1. Group delay (GD) and dispersion (D) of the microstructured fiber as a function of wavelength. Inset: microscope image of the microstructured fiber. (See Ref. 12).

^{a)}Electronic mail: mikko.lehtonen@hut.fi

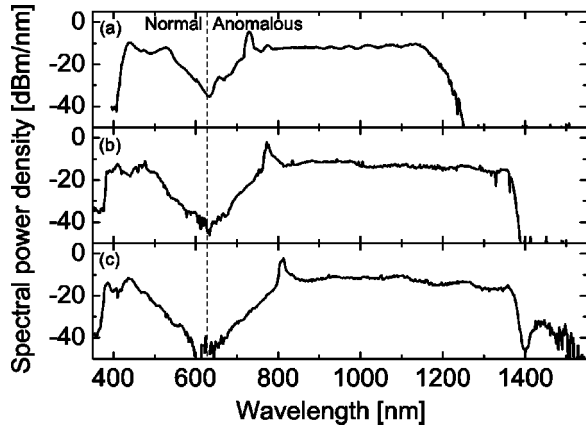


FIG. 2. Effect of pump wavelength on supercontinuum generation: (a) $\lambda_{\text{pump}} = 728$ nm, (b) $\lambda_{\text{pump}} = 771$ nm, and (c) $\lambda_{\text{pump}} = 810$ nm; $P_{\text{av}} = 35$ mW and $T_{\text{FWHM}} = 250$ fs.

and P_{av} were kept constant using a variable aperture, and the polarization of the input pulses was adjusted to match with the direction of the fast polarization axis of the fiber. The resulting spectra are shown in Fig. 2.

For a pump wavelength λ_{pump} located in the anomalous dispersion region, the extension of the continuum into the infrared is due to the initial breakup of the pulse into multiple solitons followed by a soliton self-frequency shift (SSFS). A simple model shows that the magnitude of the shift is inversely proportional to the fourth power of the width of the soliton pulse.¹³ When the pump wavelength is tuned away from the ZDW, further into the anomalous region, the temporal broadening of the multiple solitons is reduced due to the smaller cumulative dispersion. This results in an enhancement of the shift and the continuum extends further into the infrared. The bandwidth of the SC is limited by the strong OH absorption of the fiber at $1.4 \mu\text{m}$, as is observed in Fig. 2(b) for the pump wavelength of 771 nm. When the pump wavelength is increased from 771 to 810 nm, the solitons are attenuated less in the process of the SSFS, and some energy is seen to shift beyond $1.4 \mu\text{m}$.

The extension of the continuum to the blue results from the perturbation of the multiple solitons by higher-order dispersion.⁶ As the blue spectral components are matched in their group velocity with the redshifted solitons, the generation of the blue end of the continuum depends both on the pump wavelength and the dispersion profile of the fiber. In particular, the further the pump is located away from the ZDW, the further the continuum extends to the blue. This is clearly observed in Fig. 2. The gap appearing in the spectrum is determined by the GD profile of the fiber and the pump wavelength.¹⁰ When the pump is located close to the ZDW, the width of the gap becomes reduced. The magnitude of the gap is additionally decreased due to four-wave mixing. When the pump laser is tuned to longer wavelengths, the spectral separation between the solitons and the blueshifted radiation becomes larger. This reduces the four-wave-mixing gain and causes the gap to become deeper.

The effect of the polarization of the input light on the generation of the continuum was investigated at the pump wavelength tuned to 732 nm keeping P_{av} and T_{FWHM} at a constant value. The SC spectra for input polarization along the fast and slow axes are presented in Figs. 3(a) and 3(c),

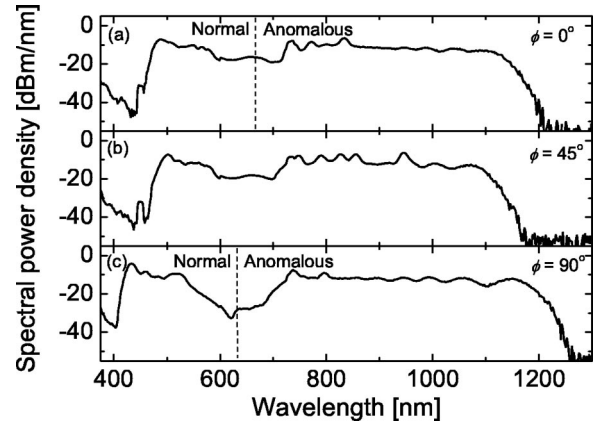


FIG. 3. Effect of input polarization on supercontinuum generation: (a) $\phi = 0^\circ$ (slow axis), (b) $\phi = 45^\circ$, and (c) $\phi = 90^\circ$ (fast axis); $P_{\text{av}} = 56$ mW and $T_{\text{FWHM}} = 200$ fs.

respectively. Figure 3(b) shows the resulting continuum for the input polarization set to an angle of $\phi = 45^\circ$ with respect to the slow axis.

When the linear polarization of the input beam matches with the direction of one of the polarization axes, the generated spectral components are found to have the same polarization as the input light. When the polarization is set to match with the direction of the fast axis, the bandwidth of the SC is observed to be broadest and the depth and width of the gap formed around the ZDW is large. Setting the polarization to match the direction of the slow axis reduces the bandwidth of the continuum as well as the gap. These observations can be explained by considering the difference in the ZDW for the two eigenpolarizations.

The pulses travel at different group velocities for the two polarizations. The minimum walk-off length can be estimated to be 6 mm for 200 fs pulses. In other words, after 6 mm of propagation, the orthogonally polarized pulses do not interact with each other any longer. Since the SC generation takes place in much longer lengths of fiber, this implies that the contribution of cross-polarization effects is negligible. For Fig. 3(b), the spectrum is a linear combination of two continua generated separately along the two principal axes of polarization in the fiber. These continua are generated with half of the total input power, which explains the decrease of the bandwidth in the measured spectrum.

We also investigated the impact of the duration of the input pulse on the SC. This was carried out by maintaining the average input power constant but altering the pulse width by adjusting a prism pair in the laser cavity. In this way, the energy of the laser pulses remains constant. The polarization was set to match with the direction of the fast axis. The spectra recorded at the output of the fiber for three different input pulse durations are shown in Fig. 4.

The formation of the continuum results from the breakup of the input pulse into multiple solitons due to Raman scattering.¹⁰ The number of the generated solitons is governed by the soliton order defined as¹⁴

$$N = \sqrt{\frac{\gamma P_p T_{\text{FWHM}}}{|\beta_2| 1.665}}, \quad (1)$$

where γ is the nonlinear coefficient of the fiber ($\gamma = 100 \text{ W}^{-1} \text{ km}^{-1}$), P_p the input peak power, T_{FWHM} the in-

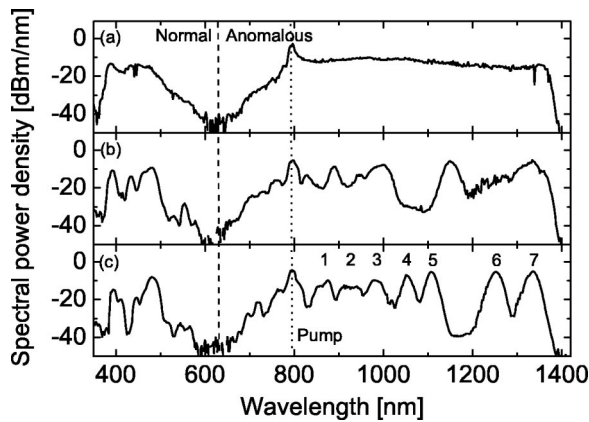


FIG. 4. Effect of input pulse duration on supercontinuum generation: (a) $T_{\text{FWHM}}=300$ fs, (b) $T_{\text{FWHM}}=100$ fs, and (c) $T_{\text{FWHM}}=70$ fs; $P_{\text{av}}=38$ mW and $\lambda_{\text{pump}}=790$ nm.

put pulse duration, and β_2 the dispersion coefficient of the fiber ($\beta_2 = -3.63 \times 10^{-23}$ s/m²). Note that by keeping the pulse energy constant and varying its duration, N varies as $\sqrt{T_{\text{FWHM}}}$. Figure 4(a) shows the output spectrum for a pulse duration of 300 fs. This corresponds to a soliton order of $N = 15$ resulting in the breakup of the pulse into 15 solitons with different amplitudes and durations.¹⁵ The center wavelengths of these solitons are redshifted due to the SSFS.

When T_{FWHM} is reduced to 100 fs, the value of the N parameter is reduced to 9 and the solitons become more clearly separated in the spectrum [Fig. 4(b)]. By further decreasing the pulse duration to 70 fs the N value is lowered to 7. In combination with the long fiber length, this value is low enough to completely distinguish the solitons in the spectrum¹⁰ [Fig. 4(c)]. Note that the blue spectral components are also more clearly separated in this case. This is a consequence of the coupling between the solitons and the blueshifted components.

To achieve an ultrabroadband continuum, we coupled 100 fs pulses at 798 nm wavelength and with ~ 140 mW average power into the MF. The polarization of the input light was adjusted to be along the direction of the fast axis. This allowed for maximizing the bandwidth of the continuum while keeping the size of the gap formed around the ZDW at an acceptable level. With these parameters, a SC spanning from 400 to 1750 nm could be generated, as illustrated in Fig. 5.

It should be possible to further increase the bandwidth of the SC by reducing the OH content of the fiber in the manufacturing process. Furthermore, since the value of the higher-order dispersion terms determines the center wavelengths of the solitons, small values should increase the magnitude of the SSFS and thereby the bandwidth of the SC. Tuning the pump wavelength closer to the ZDW reduces the amplitude

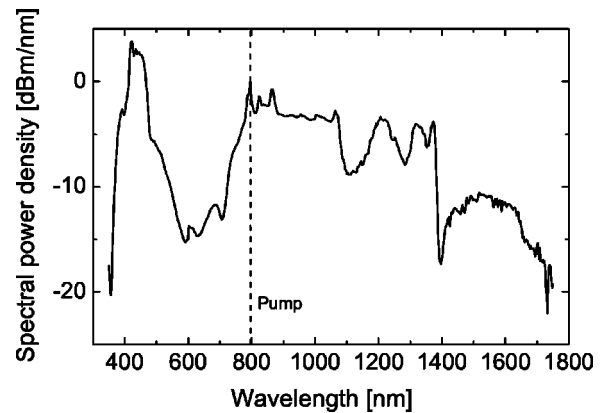


FIG. 5. Ultrabroadband supercontinuum generated in a highly birefringent microstructured fiber.

variations of the spectrum but decreases the bandwidth of the SC.

Highly birefringent microstructured fibers provide several advantages for supercontinuum generation. In particular, all the spectral components exhibit the same linear polarization and we have also found that the power required to generate the continuum is reduced compared to utilizing conventional microstructured fibers. In addition, the fiber allows for simultaneous generation of two different continua due to the large difference in group delay for the two polarization directions.

This work has been financially supported by the Academy of Finland. Crystal Fibre A/S and NKT Research are thanked for their generous loan of the fiber.

- ¹J. K. Ranka, R. S. Windeler, and A. J. Stentz, *Opt. Lett.* **25**, 25 (2000).
- ²S. T. Cundiff, J. Ye, and J. L. Hall, *Rev. Sci. Instrum.* **72**, 3749 (2001).
- ³T. Monro, W. Belardi, K. Furusawa, J. C. Baggett, N. G. Broderick, and D. J. Richardson, *Meas. Sci. Technol.* **12**, 854 (2001).
- ⁴I. Hartl, X. D. Li, C. Chudoba, R. K. Ghanta, T. H. Ko, J. G. Fujimoto, J. K. Ranka, and R. S. Windeler, *Opt. Lett.* **26**, 608 (2001).
- ⁵J. M. Dudley, L. Provino, N. Grossard, H. Maillotte, R. S. Windeler, B. J. Eggleton, and S. Coen, *J. Opt. Soc. Am. B* **19**, 765 (2002).
- ⁶A. V. Husakou and J. Herrmann, *Phys. Rev. Lett.* **87**, 203901 (2001).
- ⁷J. Herrmann, U. Griebner, N. Zhavoronkov, A. Husakou, D. Nickel, J. C. Knight, W. J. Wadsworth, P. St. J. Russell, and G. Korn, *Phys. Rev. Lett.* **88**, 173901 (2002).
- ⁸W. J. Wadsworth, A. Ortigosa-Blanch, J. C. Knight, T. A. Birks, T.-P. Martin Man, and P. St. J. Russell, *J. Opt. Soc. Am. B* **19**, 2148 (2002).
- ⁹S. Coen, A. H. L. Chau, R. Leonhardt, J. D. Harvey, J. C. Knight, W. J. Wadsworth, and P. St. J. Russell, *J. Opt. Soc. Am. B* **19**, 753 (2002).
- ¹⁰G. Genty, M. Lehtonen, H. Ludvigsen, J. Broeng, and M. Kaivola, *Opt. Express* **10**, 1083 (2002).
- ¹¹A. Ortigosa-Blanch, J. C. Knight, W. J. Wadsworth, J. Arriaga, B. J. Mangan, T. A. Birks, and P. St. J. Russell, *Opt. Lett.* **25**, 1325 (2000).
- ¹²J. Broeng, Crystal Fibre A/S (private communication).
- ¹³P. Beaud, W. Hodel, B. Zysset, and H. P. Weber, *IEEE J. Quantum Electron.* **23**, 1938 (1987).
- ¹⁴G. P. Agrawal, *Nonlinear Fiber Optics* (Academic, New York, 2001).
- ¹⁵J. K. Lucek and K. J. Blow, *Phys. Rev. A* **45**, 6666 (1992).